Kartografické listy / Cartographic letters, 2026, 34 (1), 23-46

COMPARATIVE ANALYSIS OF SELECTED DEM-BASED TERRAIN ROUGHNESS METRICS: ASSESSING THE ROLE OF LOCAL FRACTAL DIMENSION

Tomáš IČ, Renata ĎURAČIOVÁ

Comparative Analysis of Selected DEM-Based Terrain Roughness Metrics: Assessing the Role of Local Fractal Dimension

Abstract: Terrain roughness is one of the fundamental characteristics of the Earth's surface and is widely used in spatial analyses within geographic information systems (GIS). This study presents a comparative evaluation of selected methods for quantifying terrain roughness derived from raster-based digital elevation models (DEMs). Particular emphasis is placed on the local fractal dimension method, which remains underutilized in GIS environments but enables the characterization of surface geometric complexity across scales. This approach is compared with commonly used GIS-based methods relying on local elevation differences and surface orientation. The experimental analysis is conducted using three high-resolution DEM samples with a spatial resolution of 1 m. The results are presented as terrain roughness rasters and subsequently evaluated through numerical and statistical analyses. The study highlights differences among the evaluated approaches and discusses the potential of local fractal dimension as an alternative tool for terrain roughness assessment in GIS. The results indicate that the local fractal dimension provides complementary information to conventional metrics, particularly in capturing scale-dependent surface variability.

Keywords: terrain roughness, local fractal dimension (LFD), terrain ruggedness index (TRI), vector ruggedness measure (VRM), digital elevation model (DEM), GIS

Introduction

Terrain roughness is among the fundamental characteristics of the Earth's surface and represents a key parameter in geomorphometric analyses, cartographic modelling, and applications of geographic information systems (GIS). In the context of digital terrain processing, roughness is understood as a measure of the spatial variability of elevation and directional surface properties derived from a digital elevation model (DEM) (Wilson and Gallant, 2000; Pike et al., 2009). The quantification of this property plays an important role in the analysis of the morphological structure of terrain, the assessment of geomorphological processes, and in derived environmental applications (Florinsky, 2016).

In the GIS environment, several metrics have been developed to quantify surface roughness, differing in their mathematical basis, sensitivity to scale, and interpretation of results (Grohmann et al., 2011; Trevisani et al., 2012). Recent work by Trevisani and Guth (2025) emphasises that surface roughness in geomorphometry should not be treated as a single universally defined terrain property, but rather as part of a broader framework of surface texture analysis. They point out that roughness-related metrics differ in their mathematical formulation, scale sensitivity, and ability to represent specific terrain patterns, and that their interpretation depends on the selected metric, DEM resolution, analysis scale, landscape type, and research objective. This framework is particularly relevant for the present study, because parameters used, namely the local fractal dimension

Ing. Tomáš IČ, doc. Ing. Renata ĎURAČIOVÁ, PhD., Department of Theoretical Geodesy and Geoinformatics, Faculty of Civil Engineering, Slovak University of Technology in Bratislava, Radlinského 11, 810 05 Bratislava, e-mail: tomas.ic@stuba.sk, renata.duraciova@stuba.sk

(LFD), the terrain ruggedness index (TRI), and the vector ruggedness measure (VRM) are based on different concepts of terrain variability: elevation differences, surface orientation, and scale-dependent geometric complexity. Among the most commonly used methods is TRI, which was proposed as a simple index summarizing the absolute elevation differences between a central cell and its neighbouring cells within a local window of DEM (Riley et al., 1999). TRI has become one of the standard metrics of topographic heterogeneity and is widely implemented in GIS software and geomorphological studies (Pike et al., 2009; Grohmann et al., 2011).

A different concept for evaluating terrain roughness is represented by VRM, which is based on the analysis of variability in surface orientation through normal vectors derived from slope and aspect (the azimuth of the direction of the steepest slope) calculated from a DEM (Sappington et al., 2007). VRM thus represents an approach based on the orientation properties of the surface, differing from roughness indices that are directly based on elevation differences (Florinsky, 2016).

Despite their widespread use, traditional roughness indices based on local elevation or directional characteristics are often limited by a fixed analysis scale and do not provide explicit information about the multiscale complexity of the surface (Trevisani and Guth, 2025; Fan and Zhao, 2024). An alternative theoretical framework is offered by fractal geometry, which interprets natural surfaces as structures exhibiting self-similar behaviour and scale dependence, enabling their complexity to be characterised through the fractal dimension (Mandelbrot, 1982; Burrough, 1981). The fractal dimension represents a quantitative parameter describing the scale behaviour and geometric complexity of a surface, with its value expressing the degree of structural irregularity across the range of observed scales (Taud and Parrot, 2005; Gneiting et al., 2012).

The application of fractal dimension to DEM has been addressed in several studies, which have demonstrated its potential to capture terrain complexity across scales (Burrough, 1981; Taud and Parrot, 2005). Applying fractal dimension to local parts of a DEM enables the assessment of the spatial variability of surface roughness, forming the basis for the calculation of LFD within a moving window (Taud and Parrot, 2005). This approach has been further developed and applied in the GIS environment for experimental modelling of the fractal dimension of terrain and for analysing its properties (Ič, 2024).

Current literature emphasises that no single method for quantifying terrain roughness is universally applicable to all terrain types and DEM resolutions; therefore, the comparison of different approaches is justified for their proper interpretation (Grohmann et al., 2011; Fan and Zhao, 2024). This is particularly relevant for DEMs with high spatial resolution (e.g., 1 m), where different methods may emphasise different aspects of terrain structure.

The aim of this paper is to analyse approaches to the quantification of terrain roughness based on LFD and selected standard GIS methods (TRI and VRM) applied to three raster DEMs with a spatial resolution of 1 m. The analysis is carried out through visual comparison of the resulting roughness rasters and subsequent numerical and statistical evaluation, with an emphasis on identifying differences between the individual methods and their interpretative potential in GIS.

1. Methods

The quantification of terrain roughness was carried out using three methodological approaches representing different concepts of terrain complexity description. The tested methods include the LFD as a scale-adaptive fractal approach, the TRI based on local elevation differences, and the VRM, which evaluates the variability of surface orientation. All methods were applied to raster DEMs with visible elevation variability and a spatial resolution of 1 m.

1.1 Local fractal dimension

The fractal dimension represents a measure of the geometric complexity of an object, expressing a power-law relationship between the measurement scale and the scale of the object (e.g., length, area, or the number of covering elements) (Mandelbrot, 1982; Peitgen et al., 2004). In the context of terrain, fractal dimension has been applied to DEM as a tool for describing the scale variability of the surface, with several studies demonstrating its suitability for evaluating terrain roughness and texture (Burrough, 1981; Xu et al., 1993; Taud and Parrot, 2005).

Local calculations of fractal dimension over subsets of DEM presented in the literature form the basis for the concept of LFD implemented in a moving window (Taud and Parrot, 2005). This approach enables the mapping of spatial variability in terrain complexity and the identification of areas with different degrees of scale heterogeneity. In this study, the calculation of LFD is performed using the box-counting method, which is among the most commonly used approximations of fractal dimension in the analysis of raster and image data (Sun et al., 2006; Li et al., 2009; Nayak et al., 2019).

In the box-counting approach, the fractal dimension is estimated from the relationship between the size of the covering element and the number of elements required to cover the analysed object or surface (Peitgen et al., 1992). In the LFD implementation applied here, this principle is used locally within a moving window over a DEM-derived surface representation (Ič, 2024). For each local window, the surface is covered by boxes of different sizes, and the number of boxes intersecting the surface is recorded for each scale. Each iteration of the box-counting procedure yields one point in the log-log space defined by box size and the number of occupied boxes, and the resulting LFD value is estimated as the slope of the regression line fitted through these points. In this sense, LFD should be interpreted as a numerical estimate of local scale-dependent geometric complexity rather than as an exact fractal property of the terrain surface.

The LFD method applied in this paper is based on the algorithm published in the study (Ič, 2024), in which the fractal dimension is estimated locally over a raster DEM using a multilevel voxel decomposition of the surface based on the box-counting principle. For each local window with a central pixel, the surface is approximated by a triangular mesh and subsequently analysed through collision detection between triangles and voxels of different sizes corresponding to individual scales of the box-counting calculation. Intersection detection is performed using standard algorithms for triangle–box intersection (Ericson, 2005; Akenine-Möller, 2004), enabling a consistent estimation of fractal dimension while preserving the 3D geometric representation of the surface (Ič, 2024).

The triangular mesh is constructed using Delaunay triangulation (Delaunay, 1934) applied directly to the DEM grid points within each local window (Ič, 2024). Given the limited number of points in the kernel ($7\times7 = 49$), the number of meaningful scale levels is constrained, as at higher iteration levels the boxes become sufficiently small to interact primarily with the geometric properties of the interpolated triangular faces rather than with the primary elevation data, which represents a methodological limitation to be considered when selecting the number of iterations.

Before the box-counting procedure itself, a local detrending step was applied within each moving window following the approach described by Ič (2024). The coordinates of the DEM-derived local surface were transformed in order to reduce the influence of the regional planar trend, represented mainly by the inclination of the analysed window. The subsequent voxel decomposition and box-counting calculation were therefore performed on the locally transformed surface. This step is important for the interpretation of LFD, because it reduces the direct effect of the general slope or macroform of the terrain and emphasises the residual local geometric complexity of the surface.

The result of the LFD calculation is a raster in which the value of the fractal dimension expresses the degree of local geometric complexity of the surface. Higher LFD values are interpreted as an indicator of a greater degree of terrain roughness and scale heterogeneity, whereas lower values correspond to smoother and geometrically simpler surfaces (Taud and Parrot, 2005; Ič, 2024). The LFD calculation was performed using an algorithm based on the procedure described in (Ič, 2024).

1.2 Terrain ruggedness index

TRI is among the oldest and most widely used methods for quantifying terrain roughness in GIS practice. It was originally defined as the square root of the sum of squared elevation differences between the central cell of a DEM and its neighbouring cells within a local window (Riley et al., 1999):

$$TRI = \sqrt{\sum_{i=1}^{n} (z_i - z_0)^2}, \quad (1)$$

where z_o is the elevation of the central cell, z_i are the elevations of the neighbouring cells, and n is the number of cells within the window. TRI therefore directly expresses local topographic variability based on elevation contrasts. Due to this formulation, TRI exhibits a strong mathematical relationship with terrain slope, as both quantities are derived from local elevation differences between neighbouring DEM cells; consequently, TRI values tend to increase with increasing slope gradient. This slope dependency has been identified as one of the main limitations of TRI, together with its sensitivity to the fixed local neighbourhood and the different lag distances between orthogonal and diagonal directions (Trevisani et al., 2023). TRI is sensitive to the size of the selected moving window and the spatial resolution of the DEM, with smaller windows emphasising fine terrain details, whereas larger windows capture the broader structure of the terrain (Pike et al., 2009; Grohmann et al., 2011). Due to its conceptual simplicity, TRI is widely used in geomorphology, cartography, and environmental analyses (Wilson and Gallant, 2000; Florinsky, 2016).

In this study, TRI is calculated over the raster DEM using a standard square window, with the resulting output being a roughness raster representing local elevation variability of the terrain.

1.3 Vector ruggedness measure

VRM represents an alternative approach to quantifying terrain roughness based on the analysis of surface orientation. The method was proposed to describe terrain ruggedness through the variability of surface normal vectors rather than through elevation differences alone, thereby reducing the direct dependence on absolute elevation values (Sappington et al., 2007).

VRM is based on the calculation of unit normal vectors derived from slope and aspect rasters. For each DEM cell, a normal vector is defined, and within a local moving window the directional variability of these vectors is evaluated. Mathematically, the method is based on the magnitude of the resultant vector calculated from the x, y, and z components of all unit normal vectors within the window. The VRM value can be expressed as:

$$VRM = 1 - R/n, \quad (2)$$

where

$$R = \sqrt{(x_i)^2 + (y_i)^2 + (z_i)^2}, \quad (3)$$

and x_i, y_i, and z_i are the components of the unit normal vector for cell i, R is the magnitude of the resultant vector, and n is the number of cells within the moving window. If the surface normals have similar directions, R approaches n and VRM approaches 0, indicating a smooth or uniformly oriented surface. Conversely, if the normal vectors are more dispersed, R decreases and VRM increases, indicating greater local variability in surface orientation.

VRM therefore quantifies roughness as the dispersion of surface orientation rather than as local elevation variability. It is particularly sensitive to changes in slope and aspect and can capture terrain structures that may not be strongly expressed in terms of elevation differences but exhibit significant directional variability (Sappington et al., 2007; Grohmann et al., 2011; Florinsky, 2016). In this study, VRM is applied to the raster DEM, with the result being a roughness raster based on the local variability of surface orientation.

1.4 Case study

To test and compare the theoretically described methods for quantifying terrain roughness (LFD, TRI, VRM), a key step is their application to real datasets representing different types of terrain. Such experimental evaluation is commonly used in the literature to verify the robustness

and sensitivity of metrics to variability in topographic structures (Grohmann et al., 2011; Fan and Zhao, 2024). While methodological definitions provide the mathematical and conceptual basis for roughness calculation, their practical interpretation often depends on the nature of the terrain and the extent of the data to which they are applied.

The aim of the case study is to clarify how the individual methods behave in the analysis of terrain details across different morphological types, while also providing both quantitative and qualitative comparisons of their outputs. The results of this section therefore serve as a bridge between the abstract definition of the methods and their practical application to high-resolution DEM, enabling not only a visual comparison of the resulting surface ruggedness maps but also their statistical analysis with respect to areas characterised by different levels of terrain ruggedness. Such an approach reflects common practice in geomorphometric studies, where the evaluation of methods is performed on multiple independent surface samples (Grohmann et al., 2011; Fan and Zhao, 2024).

1.4.1 Study area

The experimental evaluation of terrain roughness quantification methods was carried out on three test DEM samples representing different types of terrain ruggedness. The test surfaces originate from the National Park of High Tatras and their surrounding area in northern Slovakia (Fig. 1), which represent a geomorphologically diverse mountainous environment suitable for analysing terrain complexity across multiple scales. The first two areas have an elevation difference of approximately 60 m but occur at different altitudes (representing different terrain types), while the third area has an elevation difference of only about 20 m and is located at a lower altitude. This selection of sites allows comparison of the behaviour of the tested methods under conditions of contrasting terrain forms typical of high-mountain environments.

The input data consisted of the DEM – DMR 5.0, which is the official elevation product of the Slovak Republic. The data were provided by the Geodesy, Cartography and Cadastre Authority of the Slovak Republic (GCCA SR, in Slovak ÚGKK SR) and consist of three raster subsets of the DEM with an extent of 280×280 m and a spatial resolution of 1×1 m. The DMR 5.0 was generated from a classified point cloud obtained using airborne laser scanning and is suitable for detailed geomorphometric analyses of terrain (GCCA SR, 2023).

The spatial distribution of the test sites within the territory of the Slovak Republic, as well as a detailed representation of the individual test surfaces in the form of DEM subsets, is shown in Fig. 1. The graphical representation provides spatial context for the analysed areas and simultaneously highlights differences in the morphological structure of the individual test samples that are subject to further processing and evaluation.

The visual comparison of the DEM subsets in Fig. 1 indicates differences in the morphological structure of the individual test surfaces. Surfaces 1 and 2 contain more rugged terrain forms (although located at different elevations, with an approximate difference of 800 m) compared to Surface 3, which is characterised by smoother forms due to the smaller range of elevation differences within the analysed subset. These differences create suitable conditions for analysing the sensitivity of the tested methods to different types of terrain ruggedness.

1.4.2 Derivation of terrain roughness rasters

Three different methods were used in the experiment to quantify surface roughness: LFD, TRI, and VRM. The LFD calculation was performed separately using a Python script (Ič, 2024), whereas the TRI and VRM methods were applied in the QGIS 3.32.2-Lima environment (QGIS Development Team, 2026) through the SAGA NextGen provider, which utilises external tools from SAGA GIS 9.2 (Conrad et al., 2015).

1.4.3 Comparative analysis of the applied methods for terrain roughness modelling

The mutual comparison of the outputs of the applied methods for terrain roughness modelling was performed using three complementary approaches:

– evaluation of the monotonic relationship between the resulting terrain roughness maps using Spearman's rank correlation coefficient (Spearman, 1904),

– analysis of the spatial overlap of extreme values using the Top 10 % overlap and the Jaccard index (Jaccard, 1901),
– comparison of the Z-score standardised output rasters through mapping of their differences.

The results of the case study are presented in the following sections.

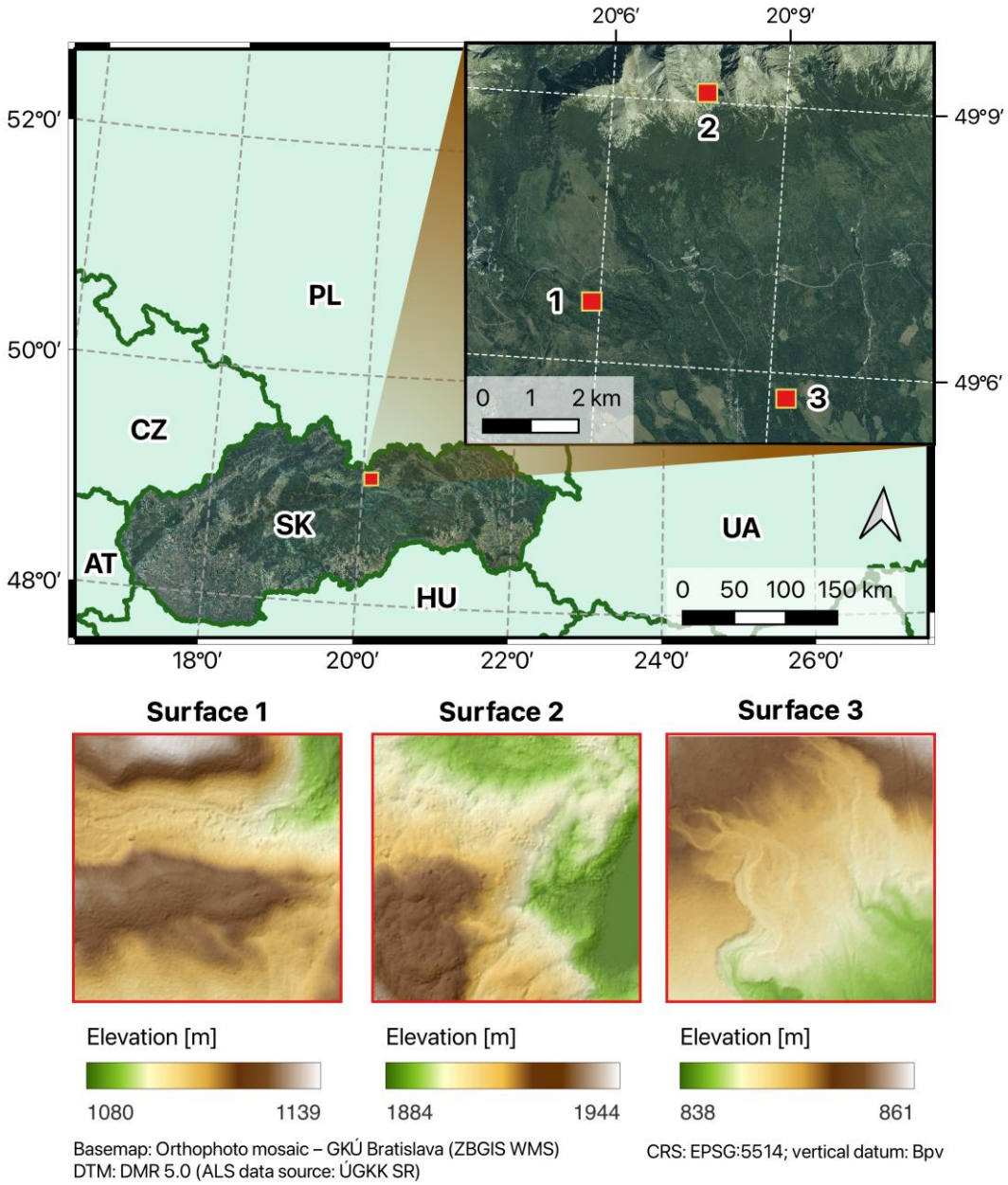

Fig. 1 Location of the test areas within the territory of the Slovak Republic and detailed representation of the three test surfaces in the form of DEM subsets

2. Results

2.1 Local fractal dimension – case study

The LFD method represents a multiscale approach to quantifying surface roughness. It allows terrain complexity to be evaluated over different computational box-size ranges depending on the number of iterations used in the calculation. In the experiment, a window radius of 3 cells was therefore used, which captures not only the immediate neighbourhood of the cell but also its broader surroundings (window = 7×7 pixels). The LFD results were evaluated after 2, 3, and 4 box-counting iterations. This setting represents a compromise between the level of captured detail and the computational cost of the algorithm, which increases exponentially with the growing number of iterations. For the given window size and DEM resolution of 1 m, the box sizes correspond to 6 m, 3 m, and 1.5 m for 2 iterations, additionally 0.75 m for 3 iterations, and further 0.375 m for 4 iterations. Such a choice of parameters makes it possible to assess how the number of box-counting iterations influences the resulting LFD values and their spatial distribution. The use of three iteration variants thus represents an assessment of the scale sensitivity of the LFD method within a fixed window, partially reflecting its multiscale character. It should be noted that there is no single optimal kernel size for characterising topographic texture (Lindsay et al., 2019). The resulting LFD rasters, preserving the spatial resolution of the input raster (1 m), are shown in Fig. 2.

The calculated LFD rasters show that higher fractal dimension values are concentrated in areas with more complex local surface geometry, which is consistent with the basic premise of the method. It should also be noted that, in the case of surfaces, the fractal dimension can theoretically take values within the range of 2–3. The graphical outputs indicate that the number of box-counting iterations influences both the spatial pattern and the distribution of LFD values. With increasing number of iterations, the occurrence of extreme high values decreases and the spatial pattern becomes more continuous. However, the interpretation of this behaviour must take into account the spatial resolution of the input DEM and the TIN-based representation of the local surface. The three-iteration case already includes a finest box size below the DEM cell size, while this limitation becomes more pronounced for four iterations, where the finest box size reaches approximately 0.375 m. Therefore, the results obtained with three and especially four iterations should be interpreted with caution, because they partly reflect the behaviour of the box-counting algorithm on the interpolated TIN surface rather than independently observed terrain detail. This issue is considered in more detail in the Discussion.

The resulting LFD rasters cover a smaller area compared to the input DEMs, as the LFD method does not allow reliable estimation of fractal dimension in the edge pixels of the input raster. The width of the marginal area without valid values corresponds to nearly half the size of the calculation window, specifically (window size − 1) / 2, which in this case results in LFD rasters with a final size of 174×174 pixels. For a more detailed assessment of the behaviour of the LFD method, Tab. 1 presents basic statistical characteristics of the resulting values, including the minimum and maximum values, the median, and the arithmetic mean.

The basic statistical characteristics indicate differences in the distribution of LFD values among the analysed surfaces. For Surface 3, the median is almost equal to the minimum LFD value and the mean value exceeds it only slightly, indicating a high concentration of low values and low internal variability of the results. In contrast, for Surfaces 1 and 2 both the mean and median values are higher, and the difference between the minimum and maximum values is more pronounced, indicating a more diverse distribution of values. Increasing the number of iterations results in a systematic decrease in the maximum values across all surfaces (e.g., for Surface 2 from 2.68 for 2 iterations to 2.46 for 3 iterations and 2.37 for 4 iterations), while the mean and median values show a gradual upward shift. For four iterations, the median values of Surfaces 1 and 2 rise above the theoretical minimum of 2.00, suggesting a broader activation of the fractal response across the surface and a more stable estimation of local geometric complexity. These trends suggest a stabilisation of the results with an increasing number of iterations and a reduced influence of extreme values while preserving the overall character of the distribution. For a clearer understanding of these relationships, Fig. 3 presents histograms of the frequency distribution of LFD values for the individual test surfaces.

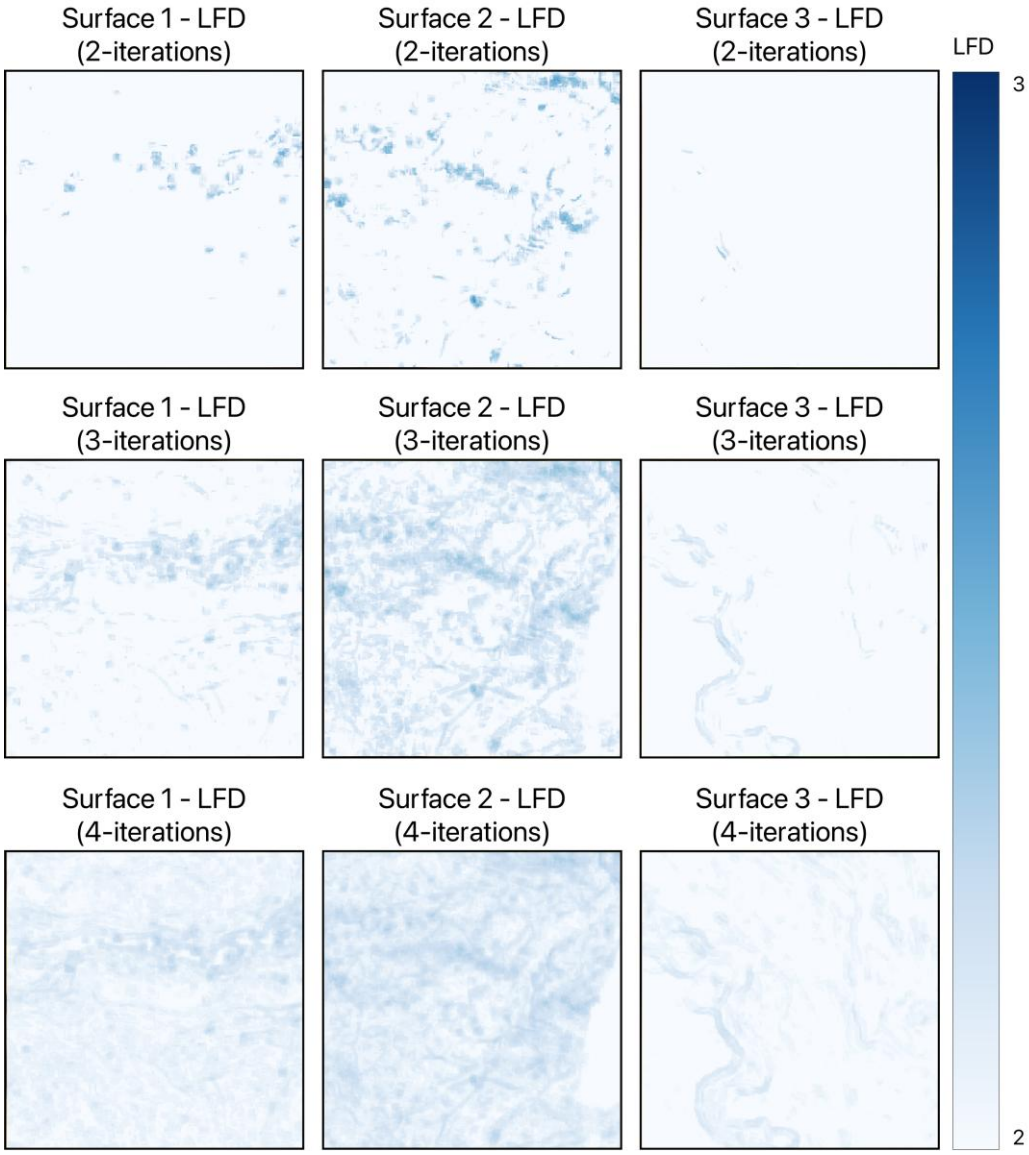

Fig. 2 Rasters of LFD for three surfaces calculated using two iterations (upper row), three iterations (middle row), and four iterations (lower row). The spatial resolution of the outputs is 1 m.

The histograms of the frequency distribution of LFD values differ among the individual surfaces primarily in the shape and concentration of their distributions. For more heterogeneous surfaces, especially Surfaces 1 and 2, the distributions are broader and include a more pronounced right-hand tail, indicating a greater occurrence of locally higher LFD values. In contrast, Surface 3 shows a stronger concentration of values close to the lower limit of the observed range, which corresponds to its smoother morphological character. Increasing the number of iterations changes the distribution of LFD values mainly by shortening the right-hand tail and reducing the occurrence of extreme high values. At the same time, the mean and, in several cases, the median values increase slightly, as shown in Table 1, indicating that the typical part of the distribution becomes more sta-

ble rather than shifting uniformly towards lower values. This behaviour suggests that additional box-counting iterations reduce the influence of isolated extreme values while producing a more continuous distribution of LFD values within the typical value range. In the interpretation of the histograms, emphasis is therefore placed primarily on the width of the distribution, the shortening of the right-hand tail, the concentration of values around the typical range, and differences among the three test surfaces.

Tab. 1 Basic statistical characteristics of the calculated LFD values for the test surfaces

		Minimum	Maximum	Median	Mean
2 iterations	Surface 1	2.00	2.58	2.00	2.01
	Surface 2	2.00	2.68	2.00	2.03
	Surface 3	2.00	2.40	2.00	2.00
3 iterations	Surface 1	2.00	2.41	2.00	2.03
	Surface 2	2.00	2.46	2.07	2.09
	Surface 3	2.00	2.30	2.00	2.01
4 iterations	Surface 1	2.00	2.33	2.06	2.07
	Surface 2	2.00	2.37	2.11	2.12
	Surface 3	2.00	2.22	2.00	2.02

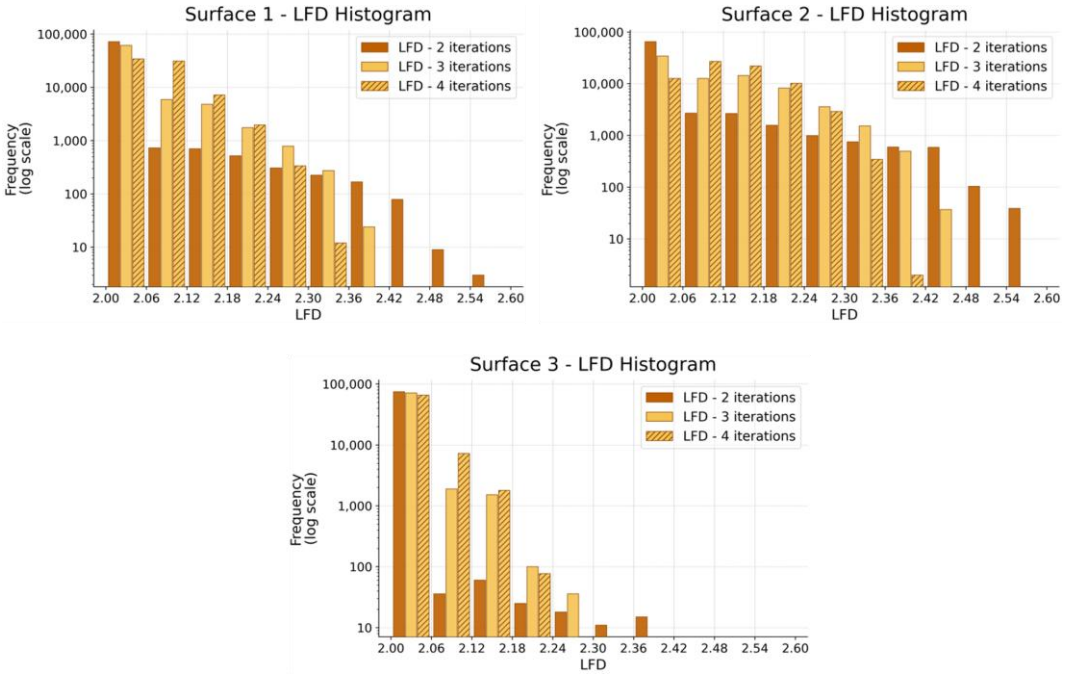

Fig. 3 Frequency histograms showing the distribution of LFD values in intervals for the test surfaces calculated using two iterations (first column), three iterations (second column), and four iterations (third column). The frequency axis is displayed on a logarithmic scale.

The reliability of the LFD estimates was assessed by evaluating the goodness of fit of the log-log regression line using the coefficient of determination (R^2) for each computation window. The R^2 value was used only as an auxiliary diagnostic indicator of the internal consistency of the local box-counting regression within the tested range of box sizes. Since the regression is based on a limited number of scale levels, specifically three points for 2 iterations, four points for 3 iterations, and five points for 4 iterations, the interpretation of R^2 must be limited to the tested range of box sizes. As shown in Fig. 4, the mean R^2 values exceed 0.99 across all three surfaces and iteration settings, indicating a consistently high linearity of the log-log relationship between box size and the number of occupied boxes.

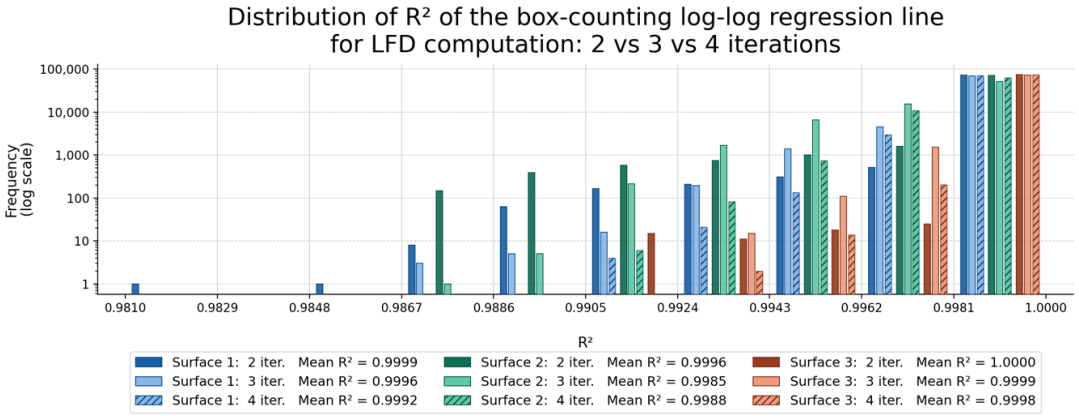

Fig. 4 Distribution of R^2 values of the log-log regression line used for LFD estimation across all computation windows for the three test surfaces and the three iteration settings: 2, 3, and 4 iterations.

The R^2 distributions reveal a consistent pattern across all three surfaces and iteration settings: the vast majority of values are concentrated close to 1, indicating a high apparent linearity of the log-log relationship between box size and the number of occupied boxes throughout the analysed area. With two iterations, the distribution shows the widest spread, with isolated values reaching down to approximately 0.981. With three iterations, the overall spread is reduced, although the distribution exhibits a somewhat more pronounced lower tail. With four iterations, the distribution is most strongly concentrated near 1. However, the interpretation of these values must be limited by the very small number of points used in the local regression: three points for 2 iterations, four points for 3 iterations, and five points for 4 iterations. Such a low number of regression points reduces the statistical robustness of the estimated slope and may lead to apparently high R^2 values. Therefore, the R^2 results should be interpreted only as an auxiliary diagnostic indicator of local regression consistency within the tested computational scale range, not as proof of a robust or universal fractal regime.

2.2 Terrain ruggedness index – case study

The quantification of terrain roughness using the TRI index represents a standard approach in GIS, based on the analysis of local elevation differences in the neighbourhood of individual cells of the raster DEM. The method enables the identification of abrupt elevation changes and thus the local variability of terrain at the microrelief scale.

In this study, the TRI calculation was performed in the QGIS environment using a tool from the SAGA module. The tool allows the configuration of basic calculation parameters, such as the size and shape of the calculation window, as well as the application of value weighting depending on the distance of cells from the centre of the moving window.

The TRI method was applied to the three test surfaces using the default parameter settings, with the search radius parameter set to 3 (window = 7×7 pixels) to ensure comparability with the

parameter configuration of the LFD method. The shape of the moving window was kept square and no weighting function was applied. Under these settings, three TRI raster outputs were obtained, which are shown in Fig. 5.

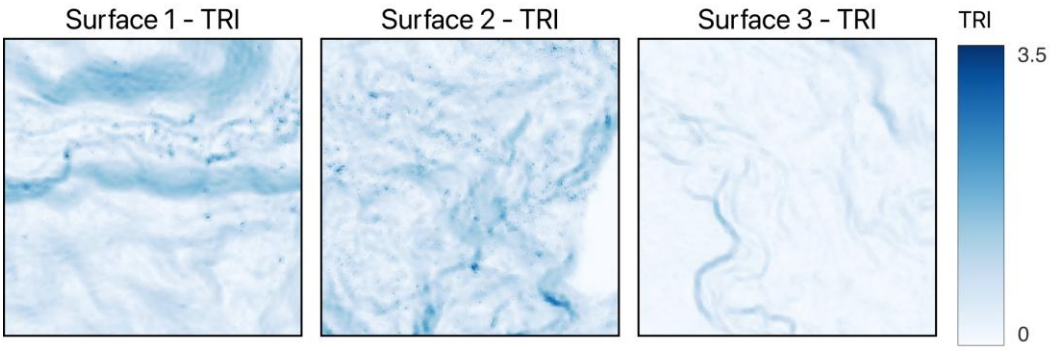

Fig. 5 The TRI rasters for the three test surfaces calculated using uniform parameter settings (square moving window with a radius of 3 cells). The outputs show the spatial distribution of local terrain variability derived from elevation differences. Spatial resolution: 1 m.

A comparison of the graphical outputs in Fig. 5 with Fig. 1 shows that the TRI index primarily highlights abrupt local changes in topography, which appear in the maps as linear and point features with higher TRI values. This effect results from the choice of a relatively small moving-window radius, within which TRI responds sensitively to pronounced elevation differences between neighbouring cells. On Surfaces 1 and 2, higher TRI values are mainly concentrated along sharp terrain transitions, breaks in slope, and more distinct microrelief features, whereas more spatially homogeneous areas exhibit low index values. Surface 3 is characterised predominantly by low TRI values, with elevated values occurring only locally, mainly in narrow linear structures, corresponding to its visually smoother terrain. The results indicate that, under the selected parameter settings, TRI effectively identifies local surface discontinuities. Basic statistical characteristics of the resulting TRI values for the individual test surfaces are presented in Tab. 2.

Tab. 2 Basic statistical characteristics of the calculated TRI values for the test surfaces

	Min.	Max.	Median	Mean
Surface 1	0.06	2.99	0.60	0.70
Surface 2	0.00	3.17	0.66	0.70
Surface 3	0.04	1.65	0.19	0.25

The basic statistical characteristics of the TRI index values indicate pronounced differences among the individual test surfaces. Surfaces 1 and 2 reach comparable mean and median values, suggesting a similar degree of local elevation variability, whereas Surface 3 is characterised by substantially lower median and mean TRI values, reflecting its overall smoother terrain (Fig. 1). The maximum TRI values are highest for Surface 2, indicating the presence of locally steep elevation changes, whereas for Surface 3 the range of values is considerably more limited. Minimum values close to zero in all cases correspond to areas with very small local elevation differences and represent a typical property of the TRI method. For a more detailed assessment of the distribution of TRI values, Fig. 6 presents histograms of the frequency distribution for the individual test surfaces.

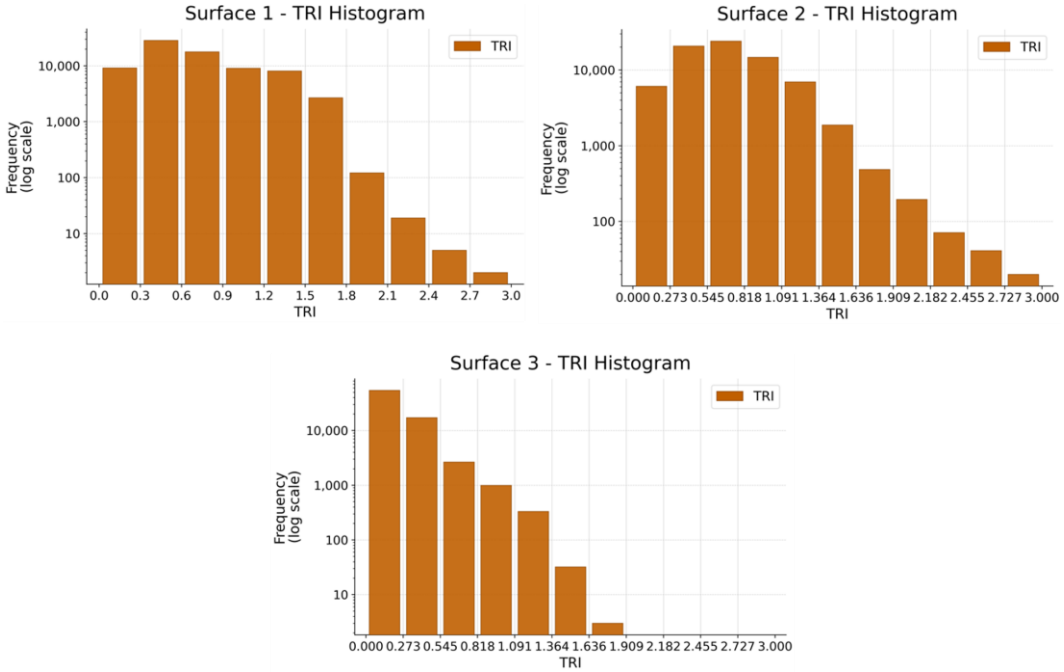

Fig. 6 Frequency histograms showing the distribution of TRI values in intervals for the individual test surfaces

The histograms of the frequency distribution of TRI values (Fig. 6) exhibit a pronounced right-skewed distribution, with a high frequency of low values dominating in all cases and a gradual decline in frequency towards higher index values. This distribution reflects the nature of the TRI method itself, which primarily responds to local elevation differences, while only a smaller proportion of cells reaches high values corresponding to abrupt topographic changes. For Surfaces 1 and 2, the distribution of values is broader, with higher TRI values occurring within a limited part of the distribution, indicating a more frequent occurrence of local steep elevation changes. In contrast, the histogram of Surface 3 is strongly concentrated in the range of low TRI values with a limited occurrence of higher values, corresponding to its overall smoother morphological character. The histograms therefore indicate that the TRI method selectively highlights only limited parts of the surface with pronounced local elevation differences, while gradual terrain changes are represented by low index values. This behaviour can be modified by increasing the size of the moving window and by applying a weighting function in the calculation.

2.3 Vector ruggedness measure – case study

The VRM method represents an approach to quantifying terrain roughness based on the analysis of the spatial variability of surface orientation. Unlike methods based directly on elevation differences, VRM is derived from the dispersion of surface normal vectors calculated from slope and aspect. It therefore does not evaluate roughness through elevation contrasts themselves, but through the local variability of surface orientation within the moving window.

In this experiment, the VRM calculation was performed in the QGIS environment using the tool from the SAGA module, which allows the derivation of surface normal vectors from raster inputs of slope and aspect and the subsequent calculation of their local variability. The tool enables the configuration of the size and shape of the moving window, as well as the definition of parameters influencing the aggregation of vector information in the neighbourhood of the analysed cell.

The VRM method was applied to the three test surfaces using the same spatial configuration of the moving window as in the LFD and TRI methods in order to ensure the comparability of the results. The moving window size was set with a radius of 3 cells (window = 7×7 pixels), and the shape of the computational unit was kept square. The application of the VRM method resulted in raster outputs in which the value represents the degree of variability in surface orientation within the local neighbourhood, with higher values indicating greater topographic complexity. The resulting VRM rasters for the individual test surfaces are shown in Fig. 7.

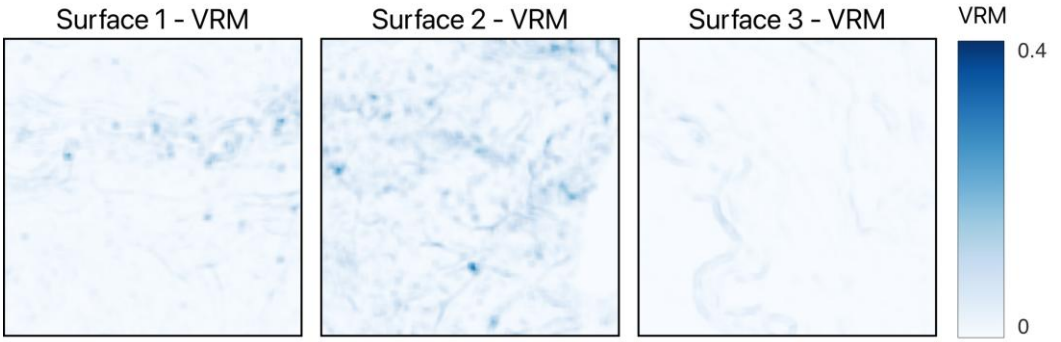

Fig. 7 Rasters of VRM values for three test surfaces computed using a uniform parameter setting (square analysis window with a radius of 3 cells). The outputs represent the spatial distribution of local variability in surface orientation. The spatial resolution of the outputs is 1 m.

The graphical outputs in Fig. 7 show that the VRM method produces predominantly very low values across most of the analysed surfaces, while higher values occur only locally and within the limited range. On Surfaces 1 and 2, elevated VRM values are mainly associated with small areal or point features corresponding to locations with more pronounced changes in surface orientation, whereas more extensive areas exhibit only minimal variability in terrain orientation. Surface 3 is characterised by an almost homogeneous distribution of very low VRM values, with higher values occurring only sporadically, corresponding to its overall smoother morphological character. The graphical outputs therefore suggest that, under the selected parameter settings, the VRM method selectively highlights only limited parts of the surface with pronounced changes in orientation, while moderate and gradual terrain variations remain less represented. These visual observations are consistent with the basic statistical characteristics of VRM values presented in Tab. 3.

Tab. 3 Basic statistical characteristics of the calculated VRM values for the test surfaces

	Minimum	Maximum	Median	Mean
Surface 1	0.00	0.21	0.01	0.02
Surface 2	0.00	0.30	0.02	0.03
Surface 3	0.00	0.10	0.00	0.01

The basic statistical characteristics of VRM values indicate a pronounced concentration of low values across all analysed surfaces. Both the median and mean VRM values are very low in all cases, suggesting that most analysed cells exhibit only a small variability of surface orientation. Surface 2 again reaches the highest maximum VRM values, in contrast to the lowest values observed for Surface 3, indicating the presence of local areas with more pronounced changes in terrain orientation. Surface 3 is also characterised by the lowest median and maximum values, corresponding to its visually smoother and less rugged terrain. Differences between the surfaces in the VRM method are therefore mainly manifested through the occurrence of sporadic higher values, while the majority of the surface remains represented by very low values of the metric. These re-

sults are followed by a more detailed assessment of the distribution of VRM values, presented as histograms of the frequency distribution for the individual test areas in Fig. 8.

The histograms of the frequency distribution of VRM values (Fig. 8) show a pronounced concentration of values close to zero in all cases, indicating the dominance of areas with low variability in surface orientation. Surfaces 1 and 2 exhibit the broader range of VRM values with occasional higher values, suggesting the presence of local areas with more pronounced changes in terrain orientation. In contrast, the histogram of Surface 3 is strongly concentrated within the narrow range of very low VRM values, while the occurrence of higher values is considerably limited. These differences in the range and concentration of values indicate that, under the selected parameter settings, the VRM method responds selectively mainly to pronounced changes in surface orientation, whereas gradual and moderate terrain variations are represented by low index values.

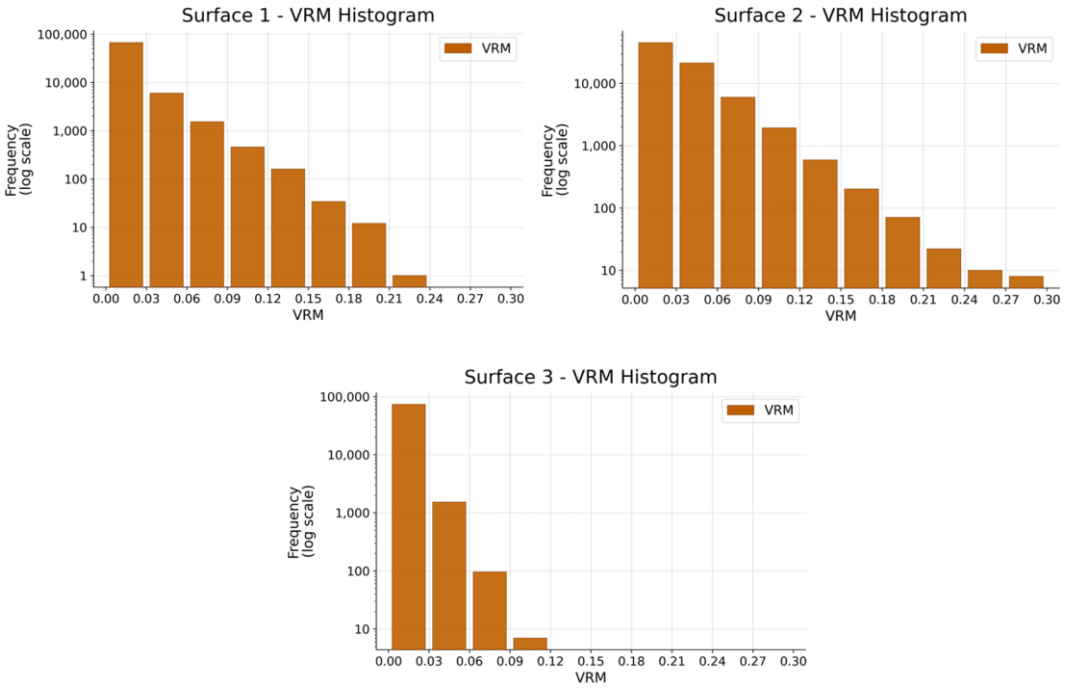

Fig. 8 Frequency histograms showing the distribution of VRM values in intervals for the individual test surfaces.

2.4 Comparative analysis of the applied methods for terrain roughness modelling – case study

The case study showed that the individual methods for quantifying terrain roughness (LFD, TRI, and VRM) respond differently to the morphological structure of the analysed surfaces and emphasise different aspects of terrain complexity. While the previous subsections focused on the individual evaluation of the behaviour of each method through visual representations, basic statistical characteristics, and histograms of values, the aim of this chapter is to analyse the obtained results and to assess the degree of agreement or difference between the tested methods.

The mutual comparison of the outputs was based on Spearman's rank correlation, spatial overlap metrics for extreme values, and differences between Z-score standardised rasters.

The selected combination of metrics makes it possible to capture not only the global statistical similarity of the outputs, but also their spatial agreement in areas with the highest degree of roughness, as well as differences in the local distribution of values.

Spearman's correlation coefficient is used to assess the monotonic relationship between terrain roughness values calculated by the individual methods without assuming linear dependence or a normal distribution of values. This approach is particularly appropriate given the strongly nonlinear nature of the analysed metrics and their differing value ranges. Additionally, an analysis of the overlap of the Top 10% of roughness values (the most rugged parts of the surface) is applied, focusing on the comparison of the spatial agreement of areas identified by the individual methods as the most pronounced in terms of terrain ruggedness. The degree of overlap is quantified using the Jaccard index, which enables an objective evaluation of the similarity of binary masks of extreme values. The results of the Spearman correlation and the Top 10% overlap analysis for the individual combinations of methods and test surfaces are presented in Tab. 4.

Tab. 4 Spearman correlation coefficients and Top 10% overlap values (Jaccard index) between the LFD, TRI, and VRM methods for the three test surfaces

		Spearman correlation coefficients			Top 10% overlap values (Jaccard index)	
		TRI	VRM		TRI	VRM
Surface 1	LFD (2it)	0.08	0.16		0.09	0.12
	LFD (3it)	0.08	0.69		0.04	0.58
	LFD (4it)		0.14	0.83	0.04	0.65
	TRI	1	0.22		1	0.06
	VRM		1			1
Surface 2	LFD (2it)	0.20	0.45		0.12	0.58
	LFD (3it)	0.30	0.89		0.11	0.55
	LFD (4it)		0.31	0.91	0.10	0.56
	TRI	1	0.42		1	0.15
	VRM		1			1
Surface 3	LFD (2it)	0.02	0.02		0.10	0.10
	LFD (3it)	0.26	0.31		0.37	0.68
	LFD (4it)		0.67	0.87	0.36	0.58
	TRI	1	0.75		1	0.41
	VRM		1			1

The results presented in Tab. 4 allow a comparison of the relationships between the individual terrain roughness quantification methods in terms of the similarity of their outputs across the entire range of values, as well as the spatial overlap of areas with the highest roughness values. Spearman's correlation coefficient expresses the degree of agreement in the ranking of values between pairs of methods, while the Top 10% overlap together with the Jaccard index evaluates the extent to which the individual methods coincide in the identification of areas with extreme roughness.

The relationship between the LFD and TRI methods is characterised by low Spearman correlation values across most combinations of surface and iteration setting, indicating that the two methods do not consistently respond to the same spatial patterns of terrain roughness. For Surfaces 1 and 2, the correlation values remain below 0.32 across all iteration settings, suggesting only a weak monotonic relationship. A notable exception is Surface 3 with four iterations, where the Spearman coefficient reaches 0.67, indicating a moderate to strong relationship, which may be related to the simpler morphological structure of this surface where both methods converge on the same limited number of locally distinct terrain features.

A comparison of the results across the three iteration settings shows that increasing the number of iterations leads to a gradual increase in the Spearman correlation between LFD and TRI across all surfaces. This pattern reflects two concurrent effects acting in opposite directions. On one hand, with a higher number of iterations the spatial ranking of LFD values becomes partly more similar to the TRI output, which may contribute to the gradual increase in correlation. On the other hand, the local detrending step removes the slope component from the LFD computation, while TRI remains directly sensitive to elevation differences. This fundamental difference keeps the overall correlation between LFD and TRI low despite the increasing number of iterations. The gradual increase in correlation with iterations can therefore be interpreted as increasing similarity in the spatial ranking of values, while the persistently low absolute correlation values reflect the conceptual divergence introduced by detrending and the different mathematical basis of both methods.

The relationship between the LFD and VRM methods shows a markedly different pattern depending on the number of iterations. For two iterations, the Spearman correlation between LFD and VRM is low across all surfaces (0.02–0.45). However, with three and four iterations the correlation increases substantially, reaching values of 0.69–0.91 for Surfaces 1 and 2 and 0.87 for Surface 3 with four iterations, indicating a strong monotonic relationship. This increasing agreement can be partly explained by a similarity between the resulting spatial patterns of the two methods that becomes more pronounced with increasing iterations: the VRM method evaluates variability of surface orientation independently of absolute elevation differences, while the local detrending step in LFD removes the dominant slope component, so that the resulting LFD pattern becomes more similar to the VRM output in terms of spatial ranking and relative distribution of values. The Jaccard index for the Top 10% overlap confirms this pattern, with values reaching 0.58–0.68 for Surfaces 1 and 3 at three and four iterations, while Surface 2 maintains consistently high overlap values across all iteration settings.

The Top 10% overlap analysis shows that despite the increasing Spearman correlation between LFD and TRI with higher iterations, the spatial overlap of extreme roughness values between these two methods remains consistently low, with Jaccard index values not exceeding 0.37 across all surfaces and iteration settings. This indicates that even when the overall ranking of values shows some agreement, the two methods do not identify the same specific locations as the most rugged. In contrast, the spatial overlap between LFD and VRM increases markedly with increasing iterations, with Jaccard values reaching 0.55–0.68 for three and four iterations across Surfaces 1, 2 and 3. The TRI vs VRM comparison yields low Jaccard values for Surfaces 1 and 2 (0.06 and 0.15) but a moderate value for Surface 3 (0.41). The results therefore confirm that the applied methods cannot be considered fully interchangeable, and their combined use provides a more comprehensive view of the structure of terrain roughness.

Since the individual methods produce values in different numerical ranges and with different distributions, direct subtraction of the original values would lead to distorted results. In the revised analysis, the output rasters were therefore standardised using Z-score transformation prior to calculating the difference maps. For each raster, the mean value was subtracted from each cell value and the result was divided by the standard deviation calculated over the common analysed area. This procedure expresses the values of each method in comparable relative units and reduces the influence of different numerical ranges between LFD, TRI, and VRM. The use of Z-score standardisation is particularly relevant for the VRM outputs, which exhibit a strongly right-skewed distribution with most values concentrated close to zero.

Based on the standardised rasters, difference maps were subsequently calculated between the individual pairs of methods, separately for each test surface. The comparisons were performed between the Z-score transformed outputs of the LFD method calculated after two, three, and four iterations, and the corresponding TRI and VRM outputs. In addition, the TRI and VRM outputs were compared with each other. The LFD outputs with different numbers of iterations were not directly compared with each other in the difference-map analysis. In total, 21 difference rasters were produced, specifically seven for each test surface. These difference maps are presented in Fig. 9.

The standardised difference rasters in Fig. 9 show that the individual roughness methods respond to terrain in different ways and highlight different spatial structures. The observed differences exhibit systematic patterns that vary with the number of LFD iterations and reflect the differing sensitivity of the compared methods to slope, surface orientation, and scale-dependent geometric complexity.

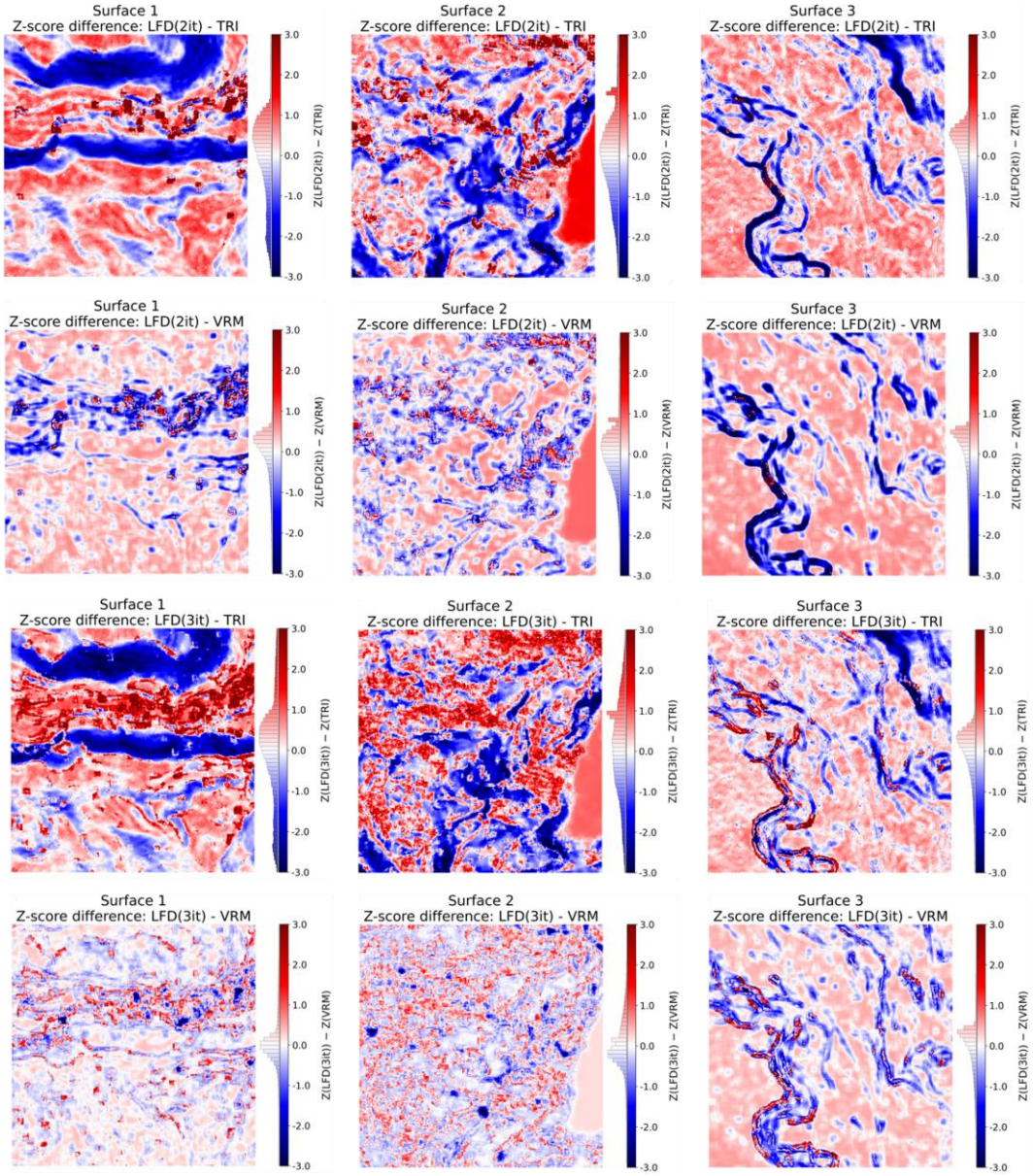

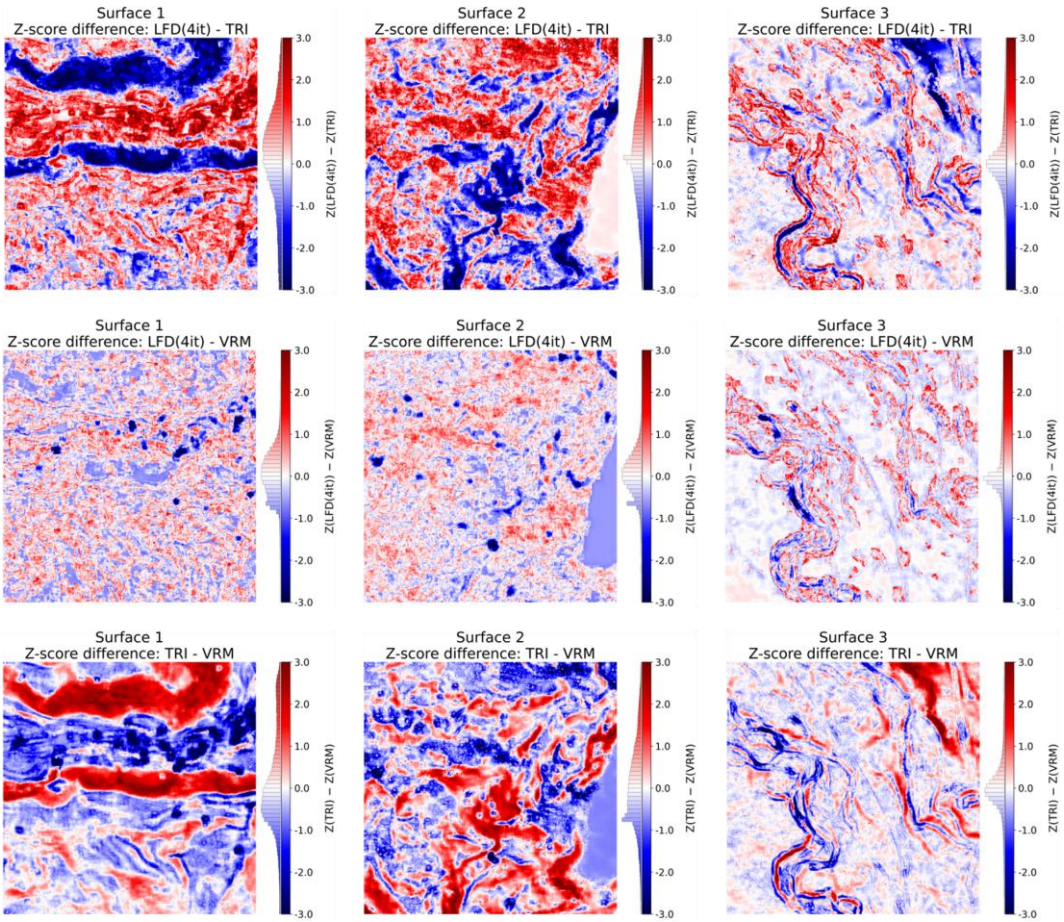

Fig. 9 Standardised difference rasters between the individual terrain roughness quantification methods (LFD, TRI, VRM) for the three test surfaces. The maps show spatial differences between pairs of methods after Z-score standardisation. Values close to zero indicate a high degree of relative agreement, whereas positive or negative deviations indicate areas where one method assigns relatively higher or lower roughness values than the other. The spatial resolution of the outputs is 1 m.

When comparing LFD with TRI, the difference maps show a spatially organised pattern with contrasting blue and red zones rather than values close to zero. Blue areas – where TRI exceeds LFD – are associated with broader banded structures corresponding to sloped terrain, where TRI responds strongly to elevation differences while LFD, through its local detrending step, increasingly suppresses the slope component with higher iterations.

Red areas – where LFD exceeds TRI – are concentrated in smaller localised linear or point-like features. With increasing iterations, this pattern becomes sharper and more detailed, although this should be interpreted as a change in the computational response of the LFD method rather than as evidence of newly resolved terrain structures. On Surface 3, the difference maps show a red background with blue values concentrated along distinct elongated linear features, indicating that TRI and LFD assign relatively higher values to different parts of these structures.

When comparing LFD with VRM, the difference maps show a different pattern. For two iterations, the maps are slightly red overall, indicating that LFD moderately exceeds VRM across most of the surface. With three and four iterations, the maps become considerably more balanced and centred around zero, indicating increasing agreement between the two methods. This increasing agreement is consistent with the high Spearman correlation values reported in Table 4 for three and four iterations and reflects a greater similarity between the standardised spatial patterns of detrended LFD and VRM. The remaining differences at higher iterations are localised and associated with narrow linear or point features rather than spatially extensive zones, making the LFD–VRM difference maps visually less contrasted than the LFD–TRI maps at equivalent iteration settings.

The direct comparison of TRI and VRM reveals systematic and spatially organised differences across all three surfaces. The difference maps show pronounced banded and elongated structures, confirming that TRI and VRM emphasise different parts of the surface. On Surfaces 1 and 2, the spatial pattern of differences corresponds to the morphological structure of the terrain visible in the DEM subsets, with TRI and VRM responding differently to sloped areas versus localised orientation changes.

It should be noted that the Z-score standardisation used in this comparison may introduce artefacts in specific situations. In areas where all methods identify pronounced roughness hotspots, the difference maps may show locally large values that are partly a consequence of the normalisation rather than true methodological disagreement, since Z-score amplifies differences between methods with very different value distributions. Additionally, on Surface 2 a flat-water surface is present in the right-central part of the area, where all methods produce near-zero roughness values. Even small absolute differences between methods in such areas can appear amplified after Z-score standardisation, which limits the direct comparability of methods with substantially different distributional properties in heterogeneous areas containing near-zero surfaces.

Across all three surfaces, the systematic character of the observed differences confirms that the divergence between methods results primarily from their differing sensitivity to slope, surface orientation, and scale-dependent geometric complexity rather than from surface-specific effects. The standardised difference maps therefore represent a complementary tool for interpreting terrain roughness, enabling the identification of areas of relative agreement and systematic differences between the applied approaches.

3. Discussion

The comparison of the LFD, TRI, and VRM methods indicates that the individual approaches do not represent terrain roughness in an identical way but rather emphasize different aspects of terrain structure. This finding is consistent with the conceptual framework proposed by Trevisani and Guth (2025), who stress that surface roughness should be interpreted as a family of surface texture descriptors rather than as a single directly comparable quantity. From this perspective, differences between LFD, TRI, and VRM should not be interpreted only as numerical disagreement, but also as a consequence of their different sensitivity to elevation variability, surface orientation, and scale-dependent geometric complexity. The results therefore support the need to select and interpret roughness metrics with respect to the scale of analysis, DEM resolution, a terrain type, and the specific purpose of the study. This interpretation also corresponds to the broader concept of geo-

morphometry, where roughness is understood as a derived characteristic dependent on the definition of the metric, the resolution of the DEM, and the scale of analysis (Wilson and Gallant, 2000; Pike et al., 2009; Wood, 1996). Several studies have also shown that changes in the input model or its resolution can significantly influence the derived roughness metrics (Hirt et al., 2010; Höfle and Rutzinger, 2011), which underlines the need to interpret results always in the context of the specific data used. A systematic test based on the aggregation of the original 1 m DEM to coarser spatial resolutions, such as 5 m or 20 m, would provide additional information on whether the observed relationship between LFD and TRI persists across different DEM resolutions; however, such an analysis represents a separate resolution-sensitivity experiment and is therefore considered a relevant direction for further research.

The relationship between LFD and TRI must be interpreted with respect to the different mathematical principles of the two methods. TRI is based on the aggregation of elevation differences within a local window (Riley et al., 1999) and is therefore strongly affected by slope-induced height variation and broader terrain form. In contrast, the LFD calculation used in this study includes a local detrending step before the box-counting procedure, which reduces the influence of the regional planar trend within the analysed window. As a result, the Spearman correlation between LFD and TRI remained low across most surfaces and iteration settings, reflecting the fundamental conceptual difference between the two methods: TRI responds directly to elevation differences driven by slope, while detrended LFD reduces the influence of the local planar trend and emphasises the remaining local geometric variability within the analysed window. The gradual increase in correlation with the number of iterations can be attributed to increasing similarity in the spatial ranking of values between LFD and TRI, while the persistently low absolute correlation values reflect the divergence introduced by detrending and by the different mathematical basis of both methods. This interpretation is consistent with the view that different roughness descriptors may emphasize different morphological features with varying sensitivity even when some spatial patterns appear similar (Grohmann et al., 2011; Fan and Zhao, 2024).

The different behaviour of VRM confirms that metrics based on surface orientation capture a different aspect of variability than metrics directly based on elevation differences (Sappington et al., 2007; Florinsky, 2016). VRM responds to the dispersion of surface normal vectors and may therefore exhibit low values even in areas with strong elevation variability, provided that the surface orientation remains relatively homogeneous. A notable finding of this study is the progressive increasing similarity between LFD and VRM outputs with increasing number of iterations, reflected in Spearman correlation values reaching 0.686–0.913 for three and four iterations. This convergence can be explained by the conceptual similarity between detrended LFD and VRM: as the local detrending step removes the dominant slope component from the LFD computation, the resulting signal increasingly reflects local variability in surface geometry independent of terrain inclination – a property that is also central to VRM. This suggests that at higher iteration settings, detrended LFD and VRM capture partially overlapping aspects of surface complexity, which has practical implications for the selection of roughness metrics in GIS-based terrain analyses.

The interpretation of the iteration effect in the LFD calculation requires particular caution. Increasing the number of box-counting iterations changes the computational scale range of the analysis, but it does not automatically mean that additional real terrain information is extracted from the DEM. The input DEM used in this study has a spatial resolution of 1 m; therefore, terrain structures below the information capacity of the original sampling cannot be treated as independently observed features. In this context, the three-iteration case is already partly limited, because its finest box size is 0.75 m, which is below the DEM cell size. This limitation becomes more pronounced for four iterations, where the finest box size reaches approximately 0.375 m. Since the local surface used in the LFD calculation is represented by a TIN constructed from DEM grid points, sub-cell box sizes interact mainly with the geometry of linearly interpolated triangular faces rather than with independently measured terrain detail. Consequently, the outputs obtained with three and especially four iterations should not be interpreted as direct evidence of real submetre microrelief structures. They should rather be understood as showing the behaviour of the LFD algorithm when the box-counting scale approaches or exceeds the information capacity of the input DEM and its TIN-based surface representation. This distinction is important because the apparent refinement of the spatial pattern may partly reflect the geometry of the interpolated surface rather than additional terrain information. These findings are consistent with the scale dependence

of fractal analysis reported in the literature (Sun et al., 2006; Nayak et al., 2019) and also support the view that roughness descriptors must be interpreted with respect to their mathematical formulation, input data resolution, and analysis scale (Trevisani and Guth, 2025).

The R^2 analysis provides an auxiliary diagnostic assessment of the local log-log regressions used for LFD estimation. The concentration of R^2 values close to 1 indicates that the fitted relationships between box size and the number of occupied boxes are internally consistent within the tested computational scale range. Nevertheless, the statistical interpretation of these values is limited by the very small number of regression points used in each local window. Depending on the number of iterations, the regression is based on only three to five points, which results in a low number of degrees of freedom and reduces the robustness of the estimated slope. High R^2 values in this context may therefore be misleading if interpreted as strong statistical evidence of a stable fractal regime. They should be understood only as an indication of internal consistency of the local box-counting regression within the tested scales. This limitation is particularly important for the three- and four-iteration cases, where the finest box sizes enter the sub-cell range and the calculation becomes increasingly influenced by the geometry of the interpolated TIN surface.

Several limitations of the present comparison should also be noted. The analysis was intentionally restricted to three selected metrics representing different conceptual approaches to terrain roughness: elevation differences, surface orientation, and scale-dependent geometric complexity. Other roughness descriptors, particularly methods based on detrending or higher-order increments such as MADk2 or the radial roughness index (RRI), could provide a more direct comparison with the detrended character of the LFD approach and should be considered in future work. This is particularly relevant because RRI was proposed as a modification of TRI designed to reduce its dependency on local slope while preserving a simple pixel-centred calculation framework (Trevisani et al., 2023). In addition, all methods were evaluated using a fixed moving-window size and the original 1 m DEM resolution. Although this setting ensured a controlled comparison under identical input conditions, the same window size in pixels should not be interpreted as a fully equivalent analytical scale for different algorithms, because each method transforms the information contained in the window in a different way. A systematic evaluation using multiple window sizes and aggregated DEM resolutions, for example 5 m and 20 m, would therefore be necessary to assess the scale sensitivity of the observed relationships among the methods, including the weak relationship between LFD and TRI and the stronger agreement between LFD and VRM at higher iteration levels.

Conclusion

The aim of this paper was to compare approaches to quantifying terrain roughness based on LFD, the TRI index, and the VRM method applied to DEMs with a resolution of 1 m. The results of the experiment demonstrated that the individual methods respond differently to the morphological structure of the terrain and emphasize different aspects of its complexity. LFD and TRI exhibited a low but gradually increasing correlation with higher number of iterations, while their spatial overlap of extreme values remained consistently low. LFD and VRM showed increasing agreement with higher iteration counts, which can be attributed to the partial similarity between detrended LFD outputs and VRM in representing local geometric variability after reducing the influence of the dominant planar trend. VRM proved to be a more selective indicator based on the variability of surface orientation.

Increasing the number of iterations in the LFD calculation confirmed the sensitivity of the method to the selected computational scale range. However, the results obtained with three and especially four iterations must be interpreted with caution, because their finest box sizes fall below the spatial resolution of the input DEM and are therefore increasingly influenced by the TIN-based interpolation of the local surface rather than by independently observed terrain detail. The findings indicate that none of the methods is universally interchangeable; however, their combined use provides a more comprehensive view of terrain roughness structure within the GIS environment. These findings may contribute to improved modelling of terrain roughness and support its application in studies where terrain morphology plays an important role, such as geomorphological and environmental analyses, hydrological modelling, and landscape process assessment.

Acknowledgments

During the preparation of this manuscript, ChatGPT was used for language editing and grammar checking. The authors reviewed and refined the generated content and assume full responsibility for the final version of the publication.

The input dataset is accessible via the following source: https://www.skgeodesy.sk/ (accessed on 29 January 2026). The data are publicly available; however, users are required to acknowledge the source as "ÚGKK SR".

Funding

This research was funded by grant No. VEGA 1/0626/25 of the Scientific Grant Agency of the Ministry of Education, Science, Research, and Sport of the Slovak Republic and the Slovak Academy of Sciences, and by the Slovak Research and Development Agency under Contract No. APVV-22-0151.

References

AKENINE-MÖLLER, T. (2004). Fast 3D Triangle-Box Overlap Testing. *Journal of Graphics Tools*, 6(1), 29-33. DOI: https://doi.org/10.1145/1198555.1198747

BURROUGH, P. A. (1981). Fractal dimensions of landscapes and other environmental data. *Nature*, 294, 240-242. DOI: 10.1038/294240a0

CONRAD, O., BECHTEL, B., BOCK, M., DIETRICH, H., FISCHER, E., GERLITZ, L., WEHBERG, J., WICHMANN, V., BÖHNER, J. (2015). System for Automated Geoscientific Analyses (SAGA) v2.1.4. *Geoscientific Model Development*, 8, 1991-2007. DOI: https://doi.org/10.5194/gmd-8-1991-2015

DELAUNAY, B. (1934). Sur la sphère vide. *Bulletin de l'Académie des Sciences de l'URSS, Classe des sciences mathématiques et naturelles*, 6, 793-800.

ERICSON, C. (2005). *Real-Time Collision Detection*. Boca Raton (CRC Press).

FAN, L., ZHAO, Y. (2024). Comparing roughness maps generated by five typical roughness descriptors for LiDAR-derived digital elevation models. *AIMS Geosciences*, 10(2), 228-241. DOI: https://doi.org/10.3934/geosci.2024013

FLORINSKY, I. V. (2016). *Digital Terrain Analysis in Soil Science and Geology*. 2nd ed. Amsterdam (Elsevier).

GNEITING, T., ŠEVČÍKOVÁ, H., PERCIVAL, D. B. (2012). Estimators of fractal dimension. *Statistical Science*, 27(2), 247-277. DOI: https://doi.org/10.1214/11-STS370

GROHMANN, C. H., SMITH, M. J., RICCOMINI, C. (2011). Multiscale Analysis of Topographic Surface Roughness in the Midland Valley, Scotland. *IEEE Transactions on Geoscience and Remote Sensing*, 49(4), 1200-1213. DOI: https://doi.org/10.1109/TGRS.2010.2053546

HIRT, C., FILMER, M. S., FEATHERSTONE, W. E. (2010). Comparison and validation of the recent freely available ASTER-GDEM ver1, SRTM ver4.1 and GEODATA DEM-9S ver3 digital elevation models over Australia. *Australian Journal of Earth Sciences*, 57(3), 337-347. DOI: https://doi.org/10.1080/08120091003677553

HÖFLE, B., RUTZINGER, M. (2011). Topographic airborne LiDAR in geomorphology: A technological perspective. *Zeitschrift für Geomorphologie*, 55(2), 1-29. DOI: https://doi.org/10.1127/0372-8854/2011/0055S2-0043

IČ, T. (2024). Local Modelling of the Fractal Dimension on Digital Elevation Models. In *Juniorstav*. Brno (FCE VUT Brno). DOI: https://doi.org/10.13164/juniorstav.2024.24061

JACCARD, P. (1901). Étude comparative de la distribution florale dans une portion des Alpes et du Jura. *Bulletin de la Société Vaudoise des Sciences Naturelles*, 37, 547-579. DOI: https://doi.org/10.5169/seals-266450

LI, J., DU, Q., SUN, C. (2009). An improved box-counting method for image fractal dimension estimation. *Pattern Recognition*, 42(11), 2460-2469. DOI: https://doi.org/10.1016/j.patcog.2009.03.001

LINDSAY, J. B., NEWMAN, D. R., FRANCIONI, A. (2019). Scale-Optimized Surface Roughness for Topographic Analysis. *Geosciences*, 9(7), 322. DOI: https://doi.org/10.3390/geosciences9070322

MANDELBROT, B. B. (1982). *The Fractal Geometry of Nature*. New York (W. H. Freeman).

NAYAK, S., MISHRA, J. R., PALAI, G. (2019). Analysing roughness of surface through fractal dimension: *A review. Image and Vision Computing*, 89, 21-34. DOI: https://doi.org/10.1016/j.imavis.2019.06.015

PEITGEN, H.-O., JÜRGENS, H., SAUPE, D. (1992). *Chaos and Fractals: New Frontiers of Science*. New York (Springer). DOI: https://doi.org/10.1007/978-1-4757-4740-9

PEITGEN, H.-O., JÜRGENS, H., SAUPE, D. (2004). *Chaos and Fractals: New Frontiers of Science*. 2nd ed. New York (Springer).

PIKE, R. J., EVANS, I. S., HENGL, T. (2009). Geomorphometry: A brief guide. *Developments in Soil Science*, 33, 3-30. DOI: https://doi.org/10.1016/S0166-2481(08)00001-9

QGIS DEVELOPMENT TEAM (2026). *QGIS Geographic Information System. Open Source Geospatial Foundation Project*. [online] [cit. 2026-01-31]. Available at: <https://qgis.org>

RILEY, S. J., DEGLORIA, S. D., ELLIOT, R. (1999). A terrain ruggedness index that quantifies topographic heterogeneity. *Intermountain Journal of Sciences*, 5(1-4), 23-27.

SAPPINGTON, J. M., LONGSHORE, K. M., THOMPSON, D. B. (2007). Quantifying landscape ruggedness for animal habitat analysis: A case study using bighorn sheep in the Mojave Desert. *Journal of Wildlife Management*, 71(5), 1419-1426. DOI: https://doi.org/10.2193/2005-723

SPEARMAN, C. (1904). The proof and measurement of association between two things. *The American Journal of Psychology*, 15(1), 72-101.

SUN, W., XU, G., GONG, P., LIANG, S. (2006). Fractal analysis of remotely sensed images: A review. *International Journal of Remote Sensing*, 27(22), 4963-4990. DOI: https://doi.org/10.1080/01431160600676695

TAUD, H., PARROT, J.-F. (2005). Measurement of DEM roughness using the local fractal dimension. *Géomorphologie*, 11(4), 327-338. DOI: https://doi.org/10.4000/geomorphologie.622

TREVISANI, S., CAVALLI, M., MARCHI, L. (2012). Surface texture analysis of a high-resolution DTM: Interpreting an alpine basin. *Geomorphology*, 161-162, 26-39. DOI: https://doi.org/10.1016/j.geomorph.2012.03.031

TREVISANI, S., TEZA, G., GUTH, P. L. (2023). Hacking the topographic ruggedness index. *Geomorphology*, 439, 108838. DOI: https://doi.org/10.1016/j.geomorph.2023.108838

TREVISANI, S., GUTH, P. L. (2025). Surface Roughness in Geomorphometry: From Basic Metrics Toward a Coherent Framework. *Remote Sensing*, 17(23), 3864. DOI: https://doi.org/10.3390/rs17233864

ÚRAD GEODÉZIE, KARTOGRAFIE A KATASTRA SLOVENSKEJ REPUBLIKY / GEODESY, CARTOGRAPHY AND CADASTRE AUTHORITY OF THE SLOVAK REPUBLIC (GCCA SR) (2026). *Digitálny model reliéfu DMR 5.0*, Bratislava (ÚGKK SR). [online] [cit. 2026-01-31]. Available at: <https://data.slovensko.sk/datasety/digitalny-model-reli%C3%A9fu-dmr-5-0>

WILSON, J. P., GALLANT, J. C. (2000). *Terrain Analysis: Principles and Applications*. New York (Wiley).

WOOD, J. (1996). *The geomorphological characterisation of digital elevation models*. PhD thesis, Leicester (University of Leicester).

XU, T., MOORE, I. D., GALLANT, J. C. (1993). Fractals, fractal dimensions and landscapes. *Geomorphology*, 8(4), 245-262. DOI: https://doi.org/10.1016/0169-555X(93)90022-T

R e s u m é

Analýza vybraných mier drsnosti reliéfu odvodených z digitálnych výškových modelov: hodnotenie významu lokálnej fraktálnej dimenzie

Článok sa zaoberá porovnávacou analýzou vybraných metrík drsnosti reliéfu odvodených z digitálnych modelov reliéfu (DMR) s vysokým rozlíšením (1 m). Drsnosť reliéfu predstavuje dôležitú charakteristiku zemského povrchu, ktorá nachádza široké uplatnenie v geomorfometrických a environmentálnych štúdiách riešených v geografických informačných systémoch (GIS). Cieľom práce je porovnať tradičné metódy hodnotenia drsnosti reliéfu s menej využívaným prístupom založeným na lokálnej fraktálnej dimenzii (LFD) a posúdiť ich interpretačný potenciál.

V štúdii sú analyzované tri hlavné prístupy: index drsnosti reliéfu (terrain ruggedness index – TRI), vektorová miera drsnosti reliéfu (vector ruggedness measure – VRM) a LFD. Index TRI je založený na rozdieloch nadmorskej výšky medzi susednými bunkami rastra, pričom efektívne identifikuje lokálne výškové zmeny. Index VRM vychádza z variability orientácie povrchu pomocou normálových vektorov a je schopný zachytiť zmeny smeru svahov nezávisle od výšky. LFD predstavuje prístup vychádzajúci z fraktálnej geometrie, ktorý umožňuje charakterizovať komplexnosť povrchu naprieč rôznymi mierkami.

Experimentálna časť bola realizovaná na troch testovacích oblastiach v oblasti Vysokých Tatier s odlišnou morfologickou štruktúrou (Obr. 1). Výsledky jednotlivých metód boli prezentované vo forme rastrov drsnosti a analyzované pomocou štatistických charakteristík, histogramov a vzájomného porovnania. Na hodnotenie vzťahov medzi metódami boli použité Spearmanov korelačný koeficient, analýza prekryvu extrémnych hodnôt (Top 10 %) a Jaccardov index, ako aj mapy rozdielov po Z-score štandardizácii dát.

Výsledky ukázali, že korelácia medzi LFD a TRI je nízka a postupne rastie s vyšším počtom iterácií, pričom priestorový prekryv extrémnych hodnôt zostáva nízky. Naopak, LFD a VRM vykazujú pri vyšších iteráciách silnú konvergenciu, čo možno vysvetliť konceptuálnou podobnosťou detrendovanej LFD a VRM pri zachytávaní geometrickej komplexnosti povrchu nezávisle od sklonu terénu. VRM sa prejavila ako selektívnejšia metóda, reagujúca najmä na zmeny orientácie povrchu.

Dôležitým aspektom je aj multimierkový charakter LFD, ktorého výsledky závisia od vstupných parametrov, najmä od počtu iterácií. Vyšší počet iterácií mení výpočtový rozsah box-counting analýzy a ovplyvňuje priestorový vzor aj distribúciu výsledných hodnôt LFD. Interpretácia týchto zmien však musí rešpektovať rozlíšenie vstupného DVM a spôsob reprezentácie povrchu pomocou TIN. Pri troch iteráciách najmenšia veľkosť boxu už klesá pod veľkosť bunky DVM a pri štyroch iteráciách sa tento subpixelový charakter výpočtu ešte zvýrazňuje. Výsledky pri troch a najmä štyroch iteráciách preto nemožno interpretovať ako zachytenie reálnych submetrových mikroreliéfnych štruktúr, ale skôr ako prejav správania sa výpočtového algoritmu na lineárne interpolovanom povrchu a ako hranicu informačnej kapacity použitej konfigurácie.

Na záver možno konštatovať, že jednotlivé metódy hodnotenia drsnosti reliéfu nie sú vzájomne zameniteľné, ale poskytujú komplementárne informácie o štruktúre terénu. Kombinácia viacerých prístupov, ako je aj zahrnutie LFD spolu s tradičnými metrikami, umožňuje komplexnejšie pochopenie variability reliéfu. Tieto poznatky sú priamo aplikovateľné napríklad v geomorfológii, environmentálnom modelovaní a analýze krajinných procesov.

Obr. 1 Poloha testovacích oblastí na území Slovenskej republiky a detailné zobrazenie troch testovacích plôch vo forme výrezov DMR

Obr. 2 Rastre lokálnej fraktálnej dimenzie (LFD) pre tri plochy vypočítané s dvoma iteráciami (horný rad), troma iteráciami (stredný rad) a štyrmi iteráciami (dolný rad). Priestorové rozlíšenie výstupov je 1 m.

Obr. 3 Histogramy početnosti hodnôt lokálnej fraktálnej dimenzie (LFD) v intervaloch pre testovacie plochy vypočítané s dvoma iteráciami (prvý stĺpec), troma iteráciami (druhý stĺpec) a štyrmi iteráciami (tretí stĺpec). Os početnosti je zobrazená v logaritmickej mierke.

Obr. 4 Distribúcia hodnôt R^2 log-log regresnej priamky použitej na odhad LFD pre všetky výpočtové okná troch testovacích plôch a tri nastavenia počtu iterácií: 2, 3 a 4 iterácie

Obr. 5 Rastre indexu drsnosti reliéfu (TRI) pre tri testovacie plochy vypočítané s jednotným nastavením parametrov (štvorcové pohyblivé okno s polomerom 3 bunky). Výstupy zobrazujú priestorové rozdelenie lokálnej variability reliéfu odvodené z výškových rozdielov. Priestorové rozlíšenie: 1 m.

Obr. 6 Histogramy početnosti hodnôt indexu drsnosti reliéfu (TRI) v intervaloch pre jednotlivé testovacie plochy

Obr. 7 Rastre hodnôt vektorovej miery drsnosti reliéfu (VRM) pre tri testovacie plochy vypočítané s jednotným nastavením parametrov (štvorcové analytické okno s polomerom 3 bunky). Výstupy predstavujú priestorové rozdelenie lokálnej variability orientácie povrchu. Priestorové rozlíšenie výstupov je 1 m.

Obr. 8 Histogramy početnosti hodnôt vektorovej miery drsnosti reliéfu (VRM) v intervaloch pre jednotlivé testovacie plochy

Obr. 9 Štandardizované rastre rozdielov medzi jednotlivými metódami kvantifikácie drsnosti reliéfu (LFD, TRI, VRM) pre tri testovacie plochy. Mapy zobrazujú priestorové rozdiely medzi dvojicami metód po Z-score štandardizácii. Hodnoty blízke nule indikujú vysokú mieru relatívnej zhody, zatiaľ čo kladné alebo záporné odchýlky označujú oblasti, v ktorých jedna metóda priraďuje relatívne vyššie alebo nižšie hodnoty drsnosti ako druhá. Priestorové rozlíšenie výstupov je 1 m.

Tab. 1 Základné štatistické charakteristiky vypočítaných hodnôt lokálnej fraktálnej dimenzie (LFD) pre testovacie plochy

Tab. 2 Základné štatistické charakteristiky vypočítaných hodnôt indexu drsnosti reliéfu (TRI) pre testovacie plochy

Tab. 3 Základné štatistické charakteristiky vypočítaných hodnôt vektorovej miery drsnosti reliéfu (VRM) pre testovacie plochy

Tab. 4 Spearmanove korelačné koeficienty a hodnoty prekryvu oblastí s 10 % najvyššími hodnotami (Jaccardov index) medzi metódami LFD, TRI a VRM pre tri testovacie plochy

Prijaté do redakcie: 20 apríla 2026
Zaradené do tlače: jún 2026